FERMILAB-PUB-16-241-PPD (accepted)

Integrated Semiconductor Quantum Dot Scintillation Detector: Ultimate Limit for Speed and Light Yield

Serge Oktyabrsky, *Senior Member, IEEE* Michael Yakimov, *Senior Member, IEEE*, Vadim Tokranov, and Pavel Murat

***Abstract*— A picosecond-range timing of charged particles and photons is a long-standing challenge for many high-energy physics, biophysics, medical and security applications. We present a design, technological pathway and challenges, and some properties important for realization of an ultrafast high-efficient room-temperature semiconductor scintillator based on self-assembled InAs quantum dots (QD) embedded in a GaAs matrix. Low QD density (<10^{15} cm^{-3}), fast (~5ps) electron capture, luminescence peak redshifted by 0.2-0.3 eV from GaAs absorption edge with fast decay time (0.5-1 ns) along with the efficient energy transfer in the GaAs matrix (4.2eV/pair) allows for fabrication of a semiconductor scintillator with the unsurpassed performance parameters. The major technological challenge is fabrication of a large volume (>1 cm^3) of epitaxial QD medium. This requires multiple film separation and bonding, likely using separate epitaxial films as waveguides for improved light coupling. Compared to traditional inorganic scintillators, the semiconductor-QD based scintillators could have about 5x higher light yield and 20x faster decay time, opening a way to gamma detectors with the energy resolution better than 1% and sustaining counting rates > 100 MHz. Picosecond-scale timing requires segmented low-capacitance photodiodes integrated with the scintillator. For photons, the proposed detector inherently provides the depth-of-interaction information.**

***Index Terms*—Optical waveguides, Quantum dots, Semiconductor radiation detectors, Solid scintillation detectors.**

I. Introduction

Although semiconductors (mostly group II-VI, such as ZnS) were among the first scintillating materials due to their high luminescence efficiency, their practical use for single particle counting is quite limited. Unlike traditional solid state scintillators with relatively deep luminescent centers, semiconductors have significantly higher self-absorption. Because of that, the propagation of the scintillation light involves multiple photon recycling events on the radiation length scale. This inevitably reduces the overall (external) efficiency and leads to a slower response. Over the years, quite a few solutions to reduce the self-absorption were proposed. In the II-VI scintillators, the major approach is based on emission from deep luminescence centers, for example in ZnSe co-doped with Te and oxygen [1] or CdS(In, Te) [2]. More technologically mature group III-V materials (such as InP and GaAs) provide significantly higher electron mobilities close to 10^4 cm^2/Vs resulting in fast capture of carriers at luminescence centers and improved response time. Recent proposals of InP scintillators employ either Burstein-Moss blue-shift of apparent optical bandgap [3] or composite "impregnated" materials consisting of multilayered quantum wells or quantum dots (QDs) embedded into III-V semiconductor [4]; the latter concept is fundamentally similar to the one described below. Due to the nature of epitaxial growth, the latter scintillators have never been produced in volumes required for practical applications.

An InAs/GaAs QD medium discussed here has unique scintillation properties as shown in Table 1. Due to inhomogeneous broadening of very narrow ground-level luminescence peaks, the self-absorption in such a medium is also very low, <1cm^{-1} for 10^{15} QDs/cm^3 [5]. Typical thickness of the epi-layer doesn't exceed several tens of microns , which is not enough to provide significant absorption for high-energy particles or photons or to contain a particle shower. Therefore, integration of multiple epi-layers into a stack becomes essential. Overall, we believe that efficient, single picosecond range timing of charged particles and photons is achievable in the proposed system. Naturally, at this time scale, the optical travel time becomes essential, in particular in semiconductors with high refractive index and low speed of light. The picosecond-scale resolution require optical paths of the order of 100 μm; therefore, a bulk scintillation detector should be partitioned into smaller pixels with individual photodetectors, and again the integration turns out to be the primary challenge. It should be noted that the QD scintillator described here was never demonstrated, and the parameters in the Table 1 are derived from the measured properties of the relevant group III-V semiconductor heterostructures.

The improvement in timing resolution could provide new capabilities in many different areas, including the time-of-

Manuscript received July 10, 2015.

S. Oktyabrsky, M. Yakimov, .V. Tokranov, are with the SUNY Colleges of Nanoscale Science and Engineering, Albany, NY 12203 USA (e-mail: soktyabrsky@sunycnse.com; myakimov@sunycnse.com; vtokranov@ sunycnse.com).

P. Murat is with Fermi National Accelerator Laboratory, Batavia, IL, 60510, USA (e-mail: murat@fnal.gov).

Color versions of one or more of the figures in this paper are available online at http://ieeexplore.ieee.org.

Operated by Fermi Research Alliance, LLC under Contract No. De-AC02-07CH11359 with the United States Department of Energy.

TABLE I
COMPARISON OF SOME FAST INORGANIC SCINTILLATORS (SOURCE: SCINTILLATOR.LBL.GOV) WITH PROJECTED PERFORMANCE OF INAS/GAAS QD SCINTILLATOR

Parameter	BaF_2	LYSO	GaAs/InAs QDs
Density (g/cm^3)	4.89	7.1	5.32
Radiation length, cm	2.03	1.1	2.3
Decay constant, ns	0.8 ns	40	1
Peak emission, nm	195; 220	428	1050
Photon Yield (photons/MeV)	1,400	34,000	240,000
Time between first photons, for 1MeV	0.57ps	1.2 ps	2 fs
Poisson-limited energy resolution at 1MeV (keV) *	62	13	4.8
Radiation hardness, Gy	10^4-10^5	10^4-10^5	$>10^4$
Coupling efficiency	<50%	<50%	~100%

*Assuming collection efficiency = 1

flight x-ray tomography or searches for new physics in final states with tau leptons.

Colloidal QD based scintillators are being currently developed [6-8]; they rely on group II-VI quantum dot powders imbedded into a host matrix, e.g. glass, organic material or liquid. Colloidal QDs operate essentially as powder phosphors. While providing high luminescence efficiency, they represent a different type of materials as compared to the single crystal InAs/GaAs QD system. In the latter, the energy absorption occurs in the matrix and emission is generated in low density QDs at wavelength, red-shifted with respect to the matrix bandgap. This reduces self-absorption and photon recycling effects detrimental for fast scintillators. Powders or colloids mostly affect the shower development. However, the emission of optical photons takes place mostly inside the QDs; as described below, electron exchange with the matrix is not essential for that.

In the following, we present a design, technological pathway and some considerations important for demonstration of an ultrafast, high-efficient room-temperature semiconductor scintillator based on InAs QDs embedded in a GaAs matrix.

II. BASIC PARAMETERS OF QD SCINTILLATOR

The basic requirements for a scintillating material include [9]: high yield of optical photons; high material density and effective atomic charge; fast decay time, durability and stability of operation parameters, as well as capabilities for required production volume and low cost. In the following, the major parameters of the best solid-state scintillators (such as lutetium-yttrium oxyorthosilicate – LYSO) will be compared with the expected performance of the QD semiconductor scintillation material.

A. Density and Photon Yield

Density of GaAs matrix, ρ=5.32 g/cm^3, and its average atomic number <Z> = 32 are basically the same as in Ge. Scintillators with density ρ>5 g/cm^3 are considered high-density materials, inorganic scintillators can have density as high as 7.1 g/cm^3 for LYSO (<Z>=20) and 8.3 g/cm^3 for $PbWO_4$.(<Z>=31). Radiation length of GaAs, X_0=2.3 cm, is very comparable to that of fast scintillators BaF_2 (X_0=2.0 cm) and CsI (X_0=1.95 cm). On the other hand, NaI(Tl) is a good example of a material, which, because of its exceptionally high light yield, has been considered as an acceptable compromise for many of applications in spite of its low density.

For an efficient detection of high energy gamma photons (>100keV), the relatively low-Z GaAs (same Z as Ge) should be a few cm thick, with Compton scattering as the dominant interaction. These drawbacks will apparently make the scintillation detector more expensive and create difficulties for calorimetry. A higher-Z semiconductor would be highly desirable, though at this time, no credible QD technology in InGaSb, TlBi or CdTe – based semiconductors, that provides similar optical properties as in GaAs, is available.

Due to the nature of high quality semiconductor crystal, InAs QDs in GaAs are expected to demonstrate very high light yield. Narrow bandgap, E_g, of GaAs is an advantage: equal amount of energy transferred to optical emission would generate more photons, resulting in lower statistical noise and better energy resolution An average excitation energy per electron-hole pair for GaAs matrix is about 2.8*E_g = 4.2 eV, or about 240,000 photons per MeV (Table 1). Typical values for currently used solid state scintillators are much lower due to their wide bandgap. High light yield in the proposed QD nanomaterial is assured by high transparency of the matrix to QD luminescence band at 1050-1150 nm that is red-shifted by 0.2-0.3 eV from the GaAs band edge energy. Low density of states and discrete atom-like spectrum results in low self-absorption by the QDs. Due to strong localization of carriers in QDs, the efficiency of QD luminescence is close to unity at room temperature and does not drop at low minority carrier densities [10].

B. Decay Time and Photon Yield

Picosecond-range timing of charged particles and high-energy photons is a long-standing challenge for many applications. In fast scintillators, the ultimate time resolution (jitter) is determined by the average time between first emitted photons (Fig. 1):

$$\Delta t = k\frac{\tau_{sc}}{N_{sc}K_{eff}}$$

with τ_{sc} – scintillator decay time, N_{sc} - scintillator photon yield (energy dependent), K_{eff} –photon detection efficiency,

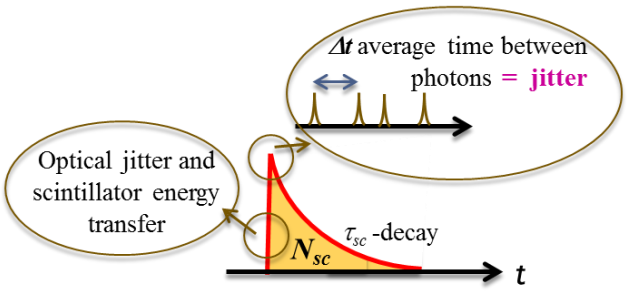

Fig. 1. Scintillator emission decay illustrating the ultimate time resolution of the system with a single photon counter.

and *k*~1(statistics dependent).

For incident particles with E ~ 1 MeV and a photon collection efficiency of ~0.2, the timing resolution of a BaF_2 or LYSO–based detector cannot be better than 3-5 ps (Table 1). The scintillator time and energy resolutions improve with the reduced scintillation time and increased photon yield. From the material choice point of view, semiconductors offer the best values for both parameters.

This brief estimation can be considered as "intrinsic" material time scale and is further affected by the scintillator geometry, photon recycling (which is very low in this material), photodetector response, etc. [11]; some of these issues are discussed in the next sections.

III. Essential Properties of InAs QDs

A. QD Formation and Electronic Spectrum

Self-assembled InAs QDs is a relatively well-studied semiconductor hetero-structure that is grown by epitaxial methods [12], such as molecular beam epitaxy (MBE) or metal-organic vapor phase epitaxy (MOVPE). Self-assembly is driven by the thermodynamics and kinetics of 2D-to-3D phase transformation on the growing surface under high biaxial compressive strain (7% for InAs on GaAs), that determine size, shape, density of QDs, and, therefore, their electronic spectrum (Fig.2). Although individual QDs offer very narrow discrete atomic-like electronic spectrum, the random nucleation and associated distribution of the QD sizes (Fig. 2b) results in inhomogeneous spectrum broadening of 40-80 nm with the peak wavelength at 1000-1100nm.

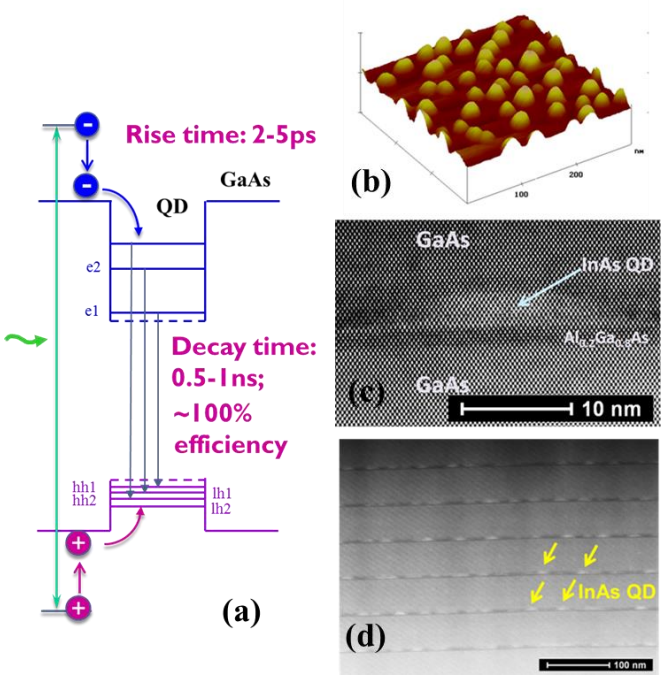

Fig. 2. (a) Schematic band-structure of InAs QDs in GaAs matrix with typical transition time scales; (b) Atomic force microscopy image of self-assembled InAs QDs on GaAs surface; (c-d) Scanning transmission electron microscopy images of a multilayer QD structure with reduced wetting layer:

Carrier dynamics is an important property for QD scintillation medium. Electrons, thermalized down to the conduction band minimum (Fig. 2a), are captured in positively charged QDs dispersed in the GaAs crystal. Due to fast electron diffusion in high-mobility GaAs matrix, the expected timescale of this process is about 2-5 ps at QD average density of ~10^{15} cm^{-3} (~10^{10} cm^{-2} in a plane with 100 nm spacing between the QD sheets) [10, 13] and can be controlled by modulation doping that creates electrostatic potential around the dots [14]. The slowest process is the QD radiation recombination (0.5-1 ns) that determines the scintillator emission time. As described in the Section II.B, for large signals, an excellent light yield in semiconductors may provide a fs-scale rise-time of a scintillating pulse.

A number of nano-engineering methods have been employed recently to control the carrier localization, electronic spectrum and carrier dynamics in QD ensembles [12]. The required relatively low density of QDs and strong localization, essential for high-efficiency luminescence, also strongly depend on the surface on which QDs form and capping layer [15-17] providing additional control options for QD density and size. Theoretical studies of correlation between QD size, shape, and electronic structure, such as ground and excited state energies are also available [18, 19] and are tested against experiment.

Other nano-engineering procedures include QD shape control [20, 21] that results in a truncated pyramid shape of QDs. This improves the electron and hole wave-function overlap and reduces the surface roughness. This structure is

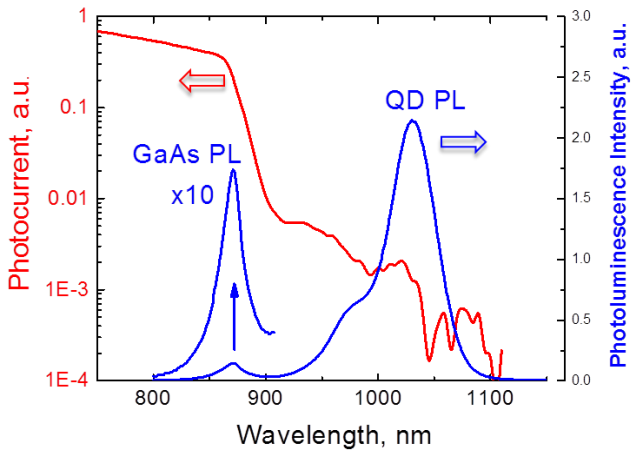

Fig. 3. Room temperature photocurrent spectra overlapped with photoluminescence (PL) spectra of the same QD structure with reduced wetting layer placed in a p-n junction. Photocurrent curve indicates that the QD luminescence peak has two orders less absorption than GaAs band-edge peak.

especially crucial for growth of multilayer stacks of QDs with more uniform strain and reduced scattering. Use of wider bandgap AlGaAs barriers around the QDs allows eliminating a wetting layer states in the bandgap. Figures 2(c-d) show a reduced wetting layer structure using 5 monolayer (ML) thick $Al_{0.2}Ga_{0.8}As$ top and bottom barriers to QDs. This approach dramatically decreases absorption by the wetting layer and

electron exchange between QDs and the matrix (Fig.3).

B. *Luminescence Efficiency and Self-Absorption*

Due to variation of the QD sizes and associated inhomogeneous broadening, the self-absorption in the QD medium can be very low and controlled by the properties of the medium. For low (<1 cm^{-1}) absorption, QDs with volume density of ~10^{15} cm^{-2} should will be used. Fig.3 plots photocurrent and photoluminescence spectra of a 20 layer QD structure in a p-n junction prepared as a QD solar cell. This structure with 8x10^{15} cm^{-3} QD density demonstrates self-absorption at 1040 nm (QD peak) about 2 orders of magnitude less than that at the 870 nm band-edge luminescence wavelength.

It should be noted that the described QD medium resembles an "ideal" scintillator based on co-doped CdS(Te,In) to produce deep luminescent centers [2]. QD electronic structure has a role of deep centers with high luminescence efficiency, fast capture and controlled density.

C. *QD Radiation Hardness*

Reliability of III-V devices was studied with respect to parameters of numerous optoelectronic and telecommunication devices deployed in the field for various applications. Protective coatings to prevent interaction with the environment, such as SiN_x or SiO_2, are well developed. A well-known challenge for semiconductor materials employing minority carrier transport is the formation of non-radiative

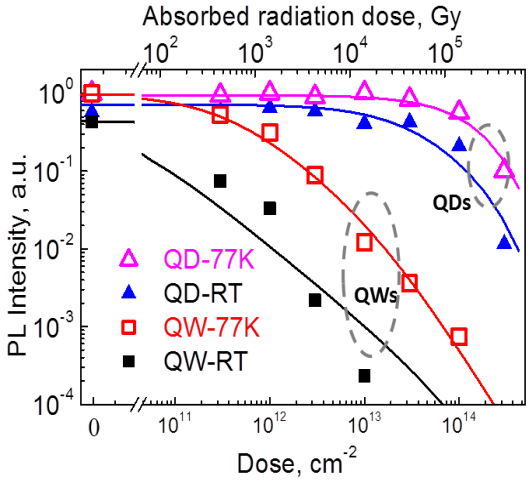

Fig. 4. Comparison of quantum well (QW) and quantum dot (QD) photoluminescence intensity at room temperature and 77K vs. 3 MeV H_2^+ implantation dose. QDs show over two orders higher radiation hardness due to strong localization of carriers in a small QD volume.

recombination centers under radiation exposure. An important property of InAs/GaAs QD systems which we recently engineered is strong localization of carriers in QDs [10]. As a consequence of fast capture to QDs and low escape probability from QDs, the interaction of carriers with defects in the GaAs matrix is significantly suppressed. It results in high radiation hardness of QD materials, significantly exceeding that of bulk semiconductors or quantum wells (Fig. 4). The demonstrated radiation hardness of >10^4 Gy (1 Mrad) is the same as in most of the inorganic solid state scintillators [22]. Strong carrier localization was also shown to provide close to unity luminescence efficiency of QD at room temperature that does not drop at low minority carrier density. These properties make this system a promising scintillator material.

IV. Optical Coupling: Wave Guiding

One of the well-recognized problems of semiconductor scintillators (as well as light-emitting diodes) is a very inefficient light extraction equal to $1/4n^2$ due to high refractive index n [23]. For the proposed InAs/GaAs QD scintillator, n = 3.4, just ~2% of light is transmitted through a planar interface with air, the rest is reflected due to total internal reflection (critical angle 17^0). Many techniques introduced to improve the light extraction range from simple epoxy cones to nanophotonic couplers. However, in many designs, the light extraction can be significantly (>10x) increased quite naturally using multiple photon recycling (self-absorption and emission) of light reflected from the surface [23]. This is a typical solution for light extraction from thick emitters with high radiative recombination efficiency [24]. Although multiple photon recycling inevitably increases the decay time, this approach can be used in semiconductor scintillators with high refractive index [25].

In the configuration with relatively thin QD layers grown by epitaxial methods, which can be treated as waveguides, a better solution is provided by light extraction from the edge of waveguide (Fig. 5a). In this case, a stack of waveguides is coupled to segmented photodiodes (PDs), which can have relatively small cross-section and capacitance. The optical transit time through the waveguide will be increased due to the relatively high effective refractive index, which depends on n and on the waveguide design. Further improvement of the photon timing could be improved by placement PDs on both sides of the waveguide, which could also provide the lateral coordinate of the absorption event [11].

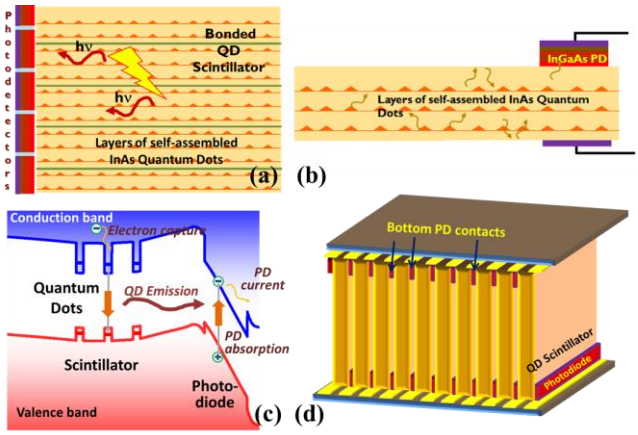

Fig. 5. (a) Multiple stacked waveguides with light extraction from the edge. (b-d) Waveguide scintillation detector with an integrated photodiode (PD) : (b) Single-layer detector layout; (c) band structure; (d) Integration of QD sheets into bulk scintillator with segmented photodetector array.

The envisioned ultimate solution for light extraction is a photodetector integrated with the scintillator (Figs. 5b-d). In

this case, the high index of refraction becomes beneficial, and the coupling efficiency between the scintillator and the PD can approach 100%. The PD typically occupies one of the scintillator faces as it has been demonstrated with ZnSe/CdSe hetero-pair [1]. For a fast response, the PD should have small capacitance and, therefore, small area that requires

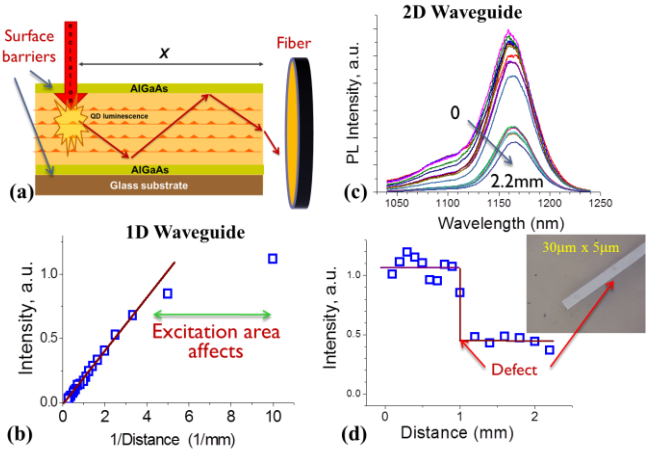

Fig. 6. Light propagation in a 5 μm thick QD waveguide (50 QD sheets x100nm): (a) Experimental setup with varying distance *x* between the photo-excitation beam and the edge; (b) PL intensity vs. *x* in a 2D waveguide; (c) PL spectra and (d) intensity vs. *x* in a 30 μm wide 1D waveguide. Inset: image of the 1D waveguide structure transferred on glass with a defect scattering light.

segmentation of the PD (Fig. 5d) and electronically combining outputs of different segments similar to that in solid-state photomultipliers. The PDs can also include avalanche sections that may be essential, in particular for detecting of low energy (1-50 keV) photons, but with the expense of increased timing jitter of about 12 ps in a 0.25 μm thick avalanche InGaAs single photon counter [26].

Light propagation in a 5 μm thick QD waveguide consisting of 50 InAs QD sheets separated by 100nm of GaAs is shown in Fig. 6. The structure was grown by MBE, separated from the GaAs substrate using epitaxial lift-off [27], and transferred on a glass substrate. The structure was modulation p-type doped to positively charge QDs for better collection of photoelectrons and contained top and bottom wide-bandgap AlGaAs barriers to prevent surface recombination of the photocarriers. Photoluminescence was excited by a scanning beam from a 532nm laser and collected into a fiber mounted at the edge of the waveguide (Fig. 6a). Fig. 6b plots the integrated PL intensity vs. inverse distance between the edge and the laser beam in a planar two-dimensional (2D) waveguide. In these coordinates, the observed linearity proves negligible absorption and scattering losses, which are not sensitive to a few defects in the structure. Figs. 6(c-d) show PL spectra and integrated intensity in a 30 μm-wide one-dimensional (1D) waveguide. In this geometry, the light propagates through the waveguide without attenuation unless a defect, which scatters the light and instantly reduces the intensity (Fig. 6d).

For few-picosecond timing, the optical travel time becomes essential, in particular in semiconductors with high refractive index and low speed of light. The device geometry should provide uncertainties in optical paths within a few 100's of μm. This may be achieved using a short waveguide with a single PD at one edge as a detector element, or longer waveguide with two PDs at the edges with differential readout [11]. In any case, a bulk scintillation detector should be partitioned into smaller elements, and integrated into one-, two- or three-dimensional arrays of pixels and, possibly, electronics, depending upon the required detector parameters (volume for high detection efficiency and/or photon timing).

V. Bulk from Epi: Technologies for Stacked Scintillator

The reviewed impressive properties of QD structures can be achieved in relatively thin epitaxial films, 10 to 50 μm at most. As stopping power and electron shower dimensions require cubic cm's of a scintillation material, a technology for producing bulk material from the epitaxial film becomes essential. In order to create the desired stack, epi-film has to be separated from the substrate and multiple layers of film have to be bonded together.

Separation of epitaxial film from a substrate, as well as bonding methods, both direct semiconductor to semiconductor, and indirect, using organic and metal adhesives, are fairly well developed. Typical applications of the film separation and transfer technologies include transfer of an epitaxial layer on a different substrate for heterogeneous integration, often a III-V device layers on a Si circuit wafer.

A method of bonding the asymmetric pairs of structures is illustrated in Fig. 7. A possible strategy utilizes bonding of the layers face-to face with simultaneous release of the bonded structure from one of the substrates which might be attached to a carrier substrate using temporary adhesive. As a result, a thicker film consisting of two bonded layers remains attached to one of the substrates. Repeating this step will result in further doubling of the thickness. The intermediate step between bonding, converting one of the two substrates to a film-release state utilizes etching to expose the sacrificial layer. Overall, after repeating process n times, a 2^n thicker film will be produced, and only 10 bonding cycles are needed to create a 1 cm thick stack starting with a 10 μm thick film.

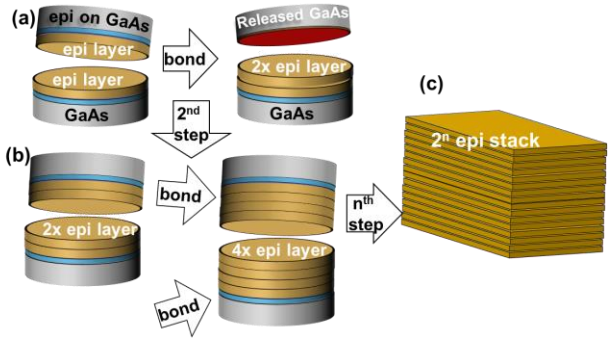

Fig. 7. Process sequence for "Bulk from Epi" technology: (a) bonding of two as-grown films: one with exposed sacrificial layer. (b) Two double-layers are bonded with sacrificial layer exposed on one side. (c) After n steps stack of 2n layers is created.

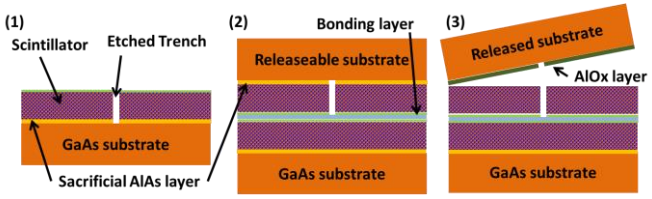

Fig. 8. Schematics of oxidation lift-off technology: (1) One of the structures are etched to expose the sacrificial AlAs layer; (2) Two structures are bonded and (3) separated from one of the GaAs substrates..

A. Substrate separation technology

Several methods of an epi-film separation from the substrate were developed for various material systems. Simple polishing/etching of the substrate to release the film is too expensive for III-V's as it does not allow for reusing of the substrate. Smart-cut^{TM} and SIMOX are most well-known due to their use in fabrication of Silicon-on-Insulator (SOI) wafers. These methods rely on the implantation of high energy ions with high temperature defect annealing – process which does not work well for III-V materials due to changes in stoichiometry and degradation of heterointerfaces.

At present, the most well-developed method for release of GaAs-based photovoltaics utilizes "epitaxial lift-off technology" [27] and is based on lateral HF etching of sacrificial AlAs epitaxial layer embedded into the structure. HF etching is known to be very selective with respect to the Al content of the AlGaAs alloy, and therefore, allows for deep lateral etching of thin embedded AlAs layers. There are a few drawbacks of the epitaxial lift-off method: it is slow with etching rate of unstressed AlAs of about 1μm/min (although under stress it can increase up to 500 μm/min [28] but might be difficult for thick film separation); it is based on wet process with associated capillary effects in narrow cavities; HF is known to preferentially etch defects (e.g. dislocations) that create large pits in the structure, and the chemistry is harmful to the environment.

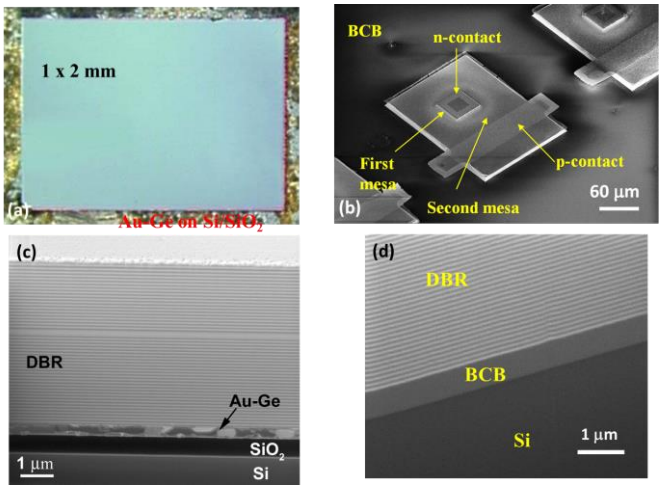

Fig. 9. (a) Large area (1x2 mm) of MBE-grown VCSEL structure transferred on Si/SiO_2 by OxLO method using Au-Ge solder bonding: 1 hour water vapor exposure at 450^{o}C; (b) VCSEL transferred using polymer BCB bonding and further processed on Si substrate; (c) and (d) secondary electron microscopy cross-section of the bonding interfaces of (a) and (b), respectively.

Another more recent technology is based on the oxidation lift-off method (OxLO) [29] which utilizes an environmental-friendly wet lateral oxidation of AlAs. The OxLO concept is illustrated in Fig. 8. The epitaxial heterostructure contains a sacrificial AlAs layer. Due to vapor-phase process the oxidation rate does not depend significantly on the thickness of the oxidation layer, as long as it is thicker than ~80 nm [29]. Prior to the OxLO integration step, trenches should be etched in the structure to expose the edge of the AlAs oxidation layer. Then the wafers with applied bonding pressure are placed in the oxidation furnace. The stack is heated to above the polymerization temperature of the polymer bonding layer or melting temperature of the solder to establish a uniform bonding. Then, the stack is heated further to the temperature of wet oxidation 400-450 °C, and exposed to an oxidation water vapor environment. The oxidation rate can be as high as 10μm/min at higher temperatures. The QD scintillator structures will likely show a higher oxidation rate due to inherent strain. During the next, cooling, step, the build-up stress developed during the oxidation of the AlAs layer produces a uniform crack along the low-density soft AlO_x layer, and the GaAs substrate is released. The substrate may be reused to grow a new QD structure.

The OxLO technology was originally developed to transfer vertical cavity surface-emitting lasers (VCSEL) on a Si wafer. We demonstrated an unsurpassed selectivity of this technology with respect to Al content to oxidize AlAs sacrificial layer and release the VCSEL structures containing $Al_xGa_{1-x}As$ layers with x = 0.9 in distributed Bragg reflectors (DBR) [29, 30]. Fig. 9(a, c) shows a 1×2 mm^2 structure transferred to a Si substrate with Au-Ge alloy bonding. The surface of the released structure is very uniform and contains a thin AlO_x layer that can be easily removed. A GaAs structure bonded to Si by benzocyclobutene (BCB)-based polymer layer and further processed to an operating device VCSEL is shown in Fig. 5(b, d). To enhance the oxidation rate, the process temperature may be increased to as high as 500 °C, but the selectivity should be tested to be appropriate for specific QD structures. As the OxLO method is based on a vapor-phase reaction, unlike the wet chemical processes, it allows very narrow trenches separating the cells and thin sacrificial layers making it possible to fabricate dense structures with minimal unused areas.

B. Bonding Technology

Bonding of multiple layers is the most critical factor in fabrication and operation of the scintillator. Bonding approaches with thicker interlayer adhesives or direct semiconductor to semiconductor bonding with monolayer-thick intermediate layers may be used. Most of the GaAs bonding so far has been done with III-V films bonded to Si chips. These approaches can also be used for GaAs-to-GaAs bonding:

1) Organic adhesive

Organic bonding adhesives, such as BCB [30] or spin-on glass, provide wide range of properties to choose from. A softer intermediate layer is advantageous for absorbing

imperfections of the wafer surface, such as dust or oval defects common for MBE-grown GaAs structures.

2) Metal bonding

Metal bonding layer (Fig. 9a,c) could be more difficult to apply as metal/semiconductor interface is typically rough which could lead to a reduced wave-guiding efficiency within a single bonded layer. However, many metal/oxide interfaces are extremely smooth and can be applied to the scintillator by deposition of a thin oxide (~10nm SiO_2) /metal bilayer with the further metal-to-metal (i.e. Au-based eutectics) bonding.

3) Direct bonding

Direct semiconductor-to-semiconductor bonding, e.g. via interdiffusion of materials at high temperature [31] or hydrophilic bonding via reaction of OH- groups [32] on both bonding surface, may be advantageous for making the stack transparent in the normal-to-layers direction. This approach could be used to manufacture the bulk material rather than layered waveguides. However, it may have a low tolerance to surface imperfections, resulting in the stack non-uniformity.

C. Stack engineering

Most properties of the proposed quasi-bulk material are preset by the epitaxial film. The primary objective of integrating multiple layers into a stack is the preservation of the film properties. Stack defects such as cracks and voids, undesired optical paths and scattering losses created in assembled structure can significantly degrade the expected material performance.

Although the target epi-layer is relatively thick (10-20 μm), the high surface recombination rate in GaAs may affect the total scintillation efficiency. In this case, modern surface and interface passivation techniques developed for novel III-V metal-oxide-semiconductor field-effect transistors become essential. For example, a 1.5nm thick amorphous Si passivation layer with 10nm thick oxide significantly reduces the interface trap density and recombination rates [33].

Combining multiple lattice mismatched layers, such as QDs, into a single crystal results in a strain. That may lead to multiple undesired effects, for example, formation of extended defects in a crystal or a mechanical deformation (bending) of the film. The latter may be a specific concern for the film separation. A single QD layer is formed by introducing about 0.5 nm of InAs into a GaAs structure. With a QD sheet spacing of 100 nm and 7% lattice mismatch between InAs and GaAs, a biaxial compressive strain of ~0.04 % can be expected in the film on the substrate. This strain will be mostly released after the film is separated from the substrate (Fig. 8) and no bending of the released layer is expected as the original strain is mostly uniform. The strain value is relatively low and will likely not affect the technology development. On the other hand, if larger dots with denser QD sheets are employed, the accumulated strain might be significantly higher. The effects of the strain can be partially mitigated by introducing layers with tensile stress, such as $GaAs_{1-x}N_x$ with x<1% [34]. The strain compensation layers would have to be engineered so that the properties of the structure are not affected by the increased absorption or recombination. That could be achieved, for example, by using AlGaAs barriers around high-recombination GaAsN to prevent carrier capture by the traps.

VI. Feasibility of Technology, Cost and Applications

The outlined design and technologies are based on three major recent developments in the integrated circuit (IC) industry: ICs have become very fast, IC technologies are very inexpensive, and III-V semiconductor materials are being introduced as IC materials, making them inexpensive too.

With recent development of 300mm and larger tool sets by VEECO (both MBE and MOCVD), Aixtron (MOCVD) and Riber (MBE), the epitaxial thin film technologies are using progressively lager substrate sizes. Since a 10μm thick film over a 300 mm wafer provides 0.7 cm^3 of material, modern reactors allow growing of a ~1cm^3 volume of the epitaxial semiconductor film in just a few hours.

Production volume and associated cost may be an issue since the epitaxial growth and III-V substrates are relatively expensive. Recent NREL analysis [35] projects a cost of $0.50/Watt for GaAs solar cells with a 3 μm thick epi-layer. The cost is mostly due to the equipment depreciation and materials (reused GaAs substrates are assumed, that is readily applicable to scintillation material). That translates into $30-50 per 1$cm^3$ of epi-film. Processing (as in solar cell industry) adds 30-50% to the material costs.

Many advanced scintillators have rare earth elements as a major component in their elemental composition. In particular, LYSO, perceived as one of the highest performance materials, is especially vulnerable to the availability of raw material: with earth crust content of <1ppm and annual world production of just around 10 tons, the stock price of lutetium was about ~$1,200/kg during 2012-2014 [36]. Due to high density of LYSO, the cost of raw material for the crystal exceeds $16 per 1$cm^3$, with LYSO prices reaching $40-50 per 1$cm^3$. On the contrary, group III-V elements are readily available in industrial quantities. These very rough numbers show that the novel scintillation nanomaterial may have a similar range of cost as quite expensive but more and more widely used LYSO.

The projected cost of the semiconductor QD scintillator becomes reasonable in view of its potential applications. An ultra-fast high-efficiency scintillator could qualitatively change fast x-ray imaging [37] and 3D imaging techniques, that rely on multiple projections (x-ray tomography, positron emission tomography-PET) [38]. Photon timing of <10 ps would provide an additional localization of photon scattering/emission event with spatial resolution close to a typical image resolution (~1mm), allowing to significantly reduce x-ray doses and detector readout times. It is worth noting, however, that PET also needs spectroscopic information for the detected photons to screen out Compton photons scattered in tissue. Therefore, PET applications will require a few cm-thick GaAs/QD stacks, and would strongly favor using a higher-Z semiconductor with the right combination of the mobility and band structure as a bulk

material for the QD-based scintillator. Picosecond-level timing can open new opportunities for particle identification in high-energy physics; high efficiency and counting rate are valuable for portable spectroscopic instruments which are now utilizing relatively slow liquid nitrogen-cooled Ge detectors.

VII. Conclusion

In conclusion, we have outlined a design and technological pathway for an integrated semiconductor scintillation detector based on InAs QDs embedded in a GaAs matrix. The approach is expected to employ III-V integration technologies into silicon ICs that are being extensively developed. The material and design promise the ultrafast timing and improved energy resolution: 5x higher scintillation yield and 20x faster decay than LYSO, which could lead to γ-detectors with energy resolution better than 1% and capable of sustaining >100 MHz counting rates.

References

[1] A. Focsha, P. Gashin, V. Ryzhikov, N. Starzhinskiy, L. Gal'chinetskii, and V. Silin, "Properties of semiconductor scintillators and combined detectors of ionizing radiation based on ZnSe (Te, O)/pZnTe–nCdSe structures," *Optical Materials*, **19**, 213-217 (2002).

[2] S. Derenzo, M. Weber, E. Bourret-Courchesne, and M. Klintenberg, "The quest for the ideal inorganic scintillator," *Nucl. Instr. Methods Phys. Res. Sect.A*, **505**, 111-117 (2003).

[3] A. Kastalsky, S. Luryi, and B. Spivak, "Semiconductor high-energy radiation scintillation detector," *Nucl. Instr. Methods Phys. Res. Sect.A*, **565**, 650-656 (2006).

[4] S. Luryi, "Impregnated semiconductor scintillator," *International Journal of High Speed Electronics and Systems*, **18**, 973-982 (2008).

[5] M. Grundmann, J. Christen, N. Ledentsov, J. Böhrer, D. Bimberg, S. Ruvimov, P. Werner, U. Richter, U. Gösele, and J. Heydenreich, "Ultranarrow luminescence lines from single quantum dots," *Phys. Rev. Lett.*, **74**, 4043 (1995).

[6] Z. Kang, Y. Zhang, H. Menkara, B. K. Wagner, C. J. Summers, W. Lawrence, and V. Nagarkar, "CdTe quantum dots and polymer nanocomposites for x-ray scintillation and imaging," *Appl. Phys. Lett.*, **98**, 181914 (2011).

[7] S. Letant and T.-F. Wang, "Semiconductor quantum dot scintillation under γ-ray irradiation," *Nano Letters*, **6**, 2877-2880 (2006).

[8] L. Winslow and R. Simpson, "Characterizing quantum-dot-doped liquid scintillator for applications to neutrino detectors," *J. Instrument.*, **7**, P07010 (2012).

[9] P. Lecoq, A. Annenkov, A. Gektin, M. Korzhik, and C. Pedrini, *Inorganic scintillators for detector systems: physical principles and crystal engineering*: Springer Science & Business Media, 2006.

[10] S. Oktyabrsky, M. Lamberti, V. Tokranov, G. Agnello, and M. Yakimov, "Room-temperature defect tolerance of band-engineered InAs quantum dot heterostructures," *J. Appl. Phys.*, **98**, 053512 (2005).

[11] S. E. Derenzo, W.-S. Choong, and W. W. Moses, "Fundamental limits of scintillation detector timing precision," *Physics in medicine and biology*, **59**, 3261 (2014).

[12] S. Oktyabrsky and A. E. Kaloyeros, "Self-Assembled Quantum Dots: Atomic Scale Engineering," in *Dekker encyclopedia of Nanoscience and Nanotechnology*, S. Lyshevski, Ed., Taylor & Francis, Boca Raton, 2014.

[13] P. Bhattacharya, S. Ghosh, S. Pradhan, J. Singh, Z.-K. Wu, J. Urayama, K. Kim, and T. B. Norris, "Carrier dynamics and high-speed modulation properties of tunnel injection InGaAs-GaAs quantum-dot lasers," *IEEE J. Quantum Electron.*, **39**, 952-962 (2003).

[14] L.-H. Chien, A. Sergeev, V. Mitin, and S. Oktyabrsky, "Quantum dot photodetectors based on structures with collective potential barriers," *OPTO*, (2010), pp. 760826-760826-8.

[15] M. Arzberger, U. Käsberger, G. Böhm, and G. Abstreiter, "Influence of a thin AlAs cap layer on optical properties of self-assembled InAs/GaAs quantum dots," *Appl. Phys. Lett.*, **75**, 3968-3970 (1999).

[16] G. Lian, J. Yuan, L. Brown, G. Kim, and D. Ritchie, "Modification of InAs quantum dot structure by the growth of the capping layer," *Appl. Phys. Lett.*, **73**, 49-51 (1998).

[17] M. Yakimov, V. Tokranov, G. Agnello, J. van Eisden, and S. Oktyabrsky, "In situ monitoring of formation of InAs quantum dots and overgrowth by GaAs or AlAs," *J. Vac. Sci. Technol. B*, **23**, 1221-1225 (2005).

[18] J. Kim, L.-W. Wang, and A. Zunger, "Comparison of the electronic structure of I n A s/G a A s pyramidal quantum dots with different facet orientations," *Phys. Rev. B*, **57**, R9408 (1998).

[19] C. Pryor, "Geometry and material parameter dependence of InAs/GaAs quantum dot electronic structure," *Phys. Rev. B*, **60**, 2869 (1999).

[20] S. Oktyabrsky, V. Tokranov, G. Agnello, J. Van Eisden, and M. Yakimov, "Nano-engineering approaches to self-assembled InAs quantum dot laser medium," *J. Electron. Mat.*, **35**, 822-833 (2006).

[21] V. Tokranov, M. Yakimov, A. Katsnelson, M. Lamberti, and S. Oktyabrsky, "Enhanced thermal stability of laser diodes with shape-engineered quantum dot medium," *Appl. Phys. Lett.*, **83**, 833-835 (2003).

[22] R. Mao, L. Zhang, and R.-Y. Zhu, "Quality of a 28 cm long LYSO crystal and progress on optical and scintillation properties," *Nuclear Science Symposium Conference Record (NSS/MIC), 2010 IEEE*, (2010), pp. 1030-1034.

[23] E. Schubert, *Light Emitting Diodes*: Cambridge University Press, 2006.

[24] I. Schnitzer, E. Yablonovitch, C. Caneau, and T. Gmitter, "Ultrahigh spontaneous emission quantum efficiency, 99.7% internally and 72% externally, from AlGaAs/GaAs/AlGaAs double heterostructures," *Appl. Phys. Lett.*, **62**, 131-133 (1993).

[25] S. Luryi and A. Subashiev, "Lévy flight of holes in InP semiconductor scintillator," *Int.J.High Speed Electronics and Systems*, **21**, 1250001 (2012).

[26] M. Yakimov, S. Oktyabrsky, and P. Murat, "Picosecond UV single photon detectors with lateral drift field: Concept and technologies," *Nucl. Instr. Methods Phys. Res. Sect.A*, **795**, 100-108 (2015).

[27] E. Yablonovitch, T. Gmitter, J. Harbison, and R. Bhat, "Extreme selectivity in the lift-off of epitaxial GaAs films," *Appl. Phys. Lett.*, **51**, 2222-2224 (1987).

[28] J. J. Schermer, P. Mulder, G. J. Bauhuis, M. M. A. J. Voncken, J. van Deelen, E. Haverkamp, and P. K. Larsen, "Epitaxial Lift-Off for large area thin film III/V devices," *Phys. Status Sol. (a)*, **202**, 501-508 (2005).

[29] S. Oktyabrsky, A. Katsnelson, V. Tokranov, R. Todt, and M. Yakimov, "Oxidation lift-off method for layer transfer of GaAs/AlAs-based structures," *Appl. Phys. Lett.*, **85**, 151-153 (2004).

[30] A. Katsnelson, V. E. Tokranov, M. Yakimov, M. Lamberti, and S. Oktyabrsky, "Hybrid integration of III-V optoelectronic devices on Si platform using BCB," *Proc. SPIE*, **4997**, 198-205 (2003).

[31] H. Wada, Y. Ogawa, and T. Kamijoh, "Electrical characteristics of directly-bonded GaAs and InP," *Appl. Phys. Lett.*, **62**, 738-740 (1993).

[32] T. Izuhara, M. Levy, and R. Osgood Jr, "Direct wafer bonding and transfer of 10-μm-thick magnetic garnet films onto semiconductor surfaces," *Appl. Phys. Lett.*, **76**, 1261-1263 (2000).

[33] S. Oktyabrsky, Y. Nishi, S. Koveshnikov, W.-E. Wang, N. Goel, and W. Tsai, "Materials and Technologies for III-V MOSFETs," in *Fundamentals of III-V Semiconductor MOSFETs*, S. Oktyabrsky and P. Ye, Eds., Springer US, 2010, pp. 195-250.

[34] Y. Okada, R. Oshima, and A. Takata, "Characteristics of InAs/GaNAs strain-compensated quantum dot solar cell," *J. Appl. Phys.*, **106**, 024306 (2009).

[35] M. Woodhouse and A. Goodrich, "Manufacturing Cost Analysis Relevant to Single and Dual-Junction Photovoltaic Cells Fabricated with III-Vs and III-Vs Grown on Silicon " NREL report PR-6A20-601262013.

[36] M. A. Müller, D. Schweizer, and V. Seiler. (November 13, 2014). *Wealth Effects of Rare Earth Prices and China's Rare Earth Elements Policy* Available: http://ssrn.com/abstract=2524148.

[37] Z. Wang, C. L. Morris, J. S. Kapustinsky, K. Kwiatkowski, and S.-N. Luo, "Towards hard x-ray imaging at GHz frame ratea)," *Rev. Sci. Instrum.*, **83**, 10E510 (2012).

[38] M. Conti, L. Eriksson, H. Rothfuss, and C. L. Melcher, "Comparison of Fast Scintillators With TOF PET Potential," *IEEE Trans. Nuclear Sci.*, **56**, 926-933 (2009).